

Monitoring fluctuations at a synchrotron beamline using matched ion chambers: 1. modelling, data collection, and deduction of simple measures of association

C. T. Chantler,^{1*} C. Q. Tran,¹ D. Paterson,¹ Z. Barnea¹ and D. J. Cookson²

¹ School of Physics, University of Melbourne, Parkville, Victoria 3010, Australia

² Australian Nuclear Science and Technology Organisation, Private Mail Bag 1, Menai, NSW 2234, Australia and Chem-Mat-CARS-CAT (Sector 15, Bldg 434D), Argonne National Laboratory, 9700 S. Cass Avenue, Argonne, Illinois 60439, USA

The flux, brightness and temporal characteristics of an x-ray source often define its utility for a specific experiment. However, there are numerous contributions to the statistics of a beam as observed by a particular detector and associated electronics. The significance of these fluctuations is often neglected, with a consequent loss of precision or accuracy of up to two orders of magnitude. An understanding of the detected statistics for a given arrangement (and the means for optimizing this) can make the difference between a successful experiment and a much more limited investigation. We explain the method for measuring a wide variety of important statistical contributions to high accuracy, and draw attention to the statistical consequences of optimized monitoring of upstream signals. We discuss the use of two matched ion chambers on a monochromatized bending magnet beam at the Photon Factory, Tsukuba, Japan. This is an illustration of a general principle, also applicable to conventional fixed x-ray sources, for investigating simple measures of association. It allows the quantification of uncertainties of spectrometric measurements, and also allows these to be minimized. Copyright © 2000 John Wiley & Sons, Ltd.

INTRODUCTION

Synchrotrons yield the brightest and strongest fluxes of x-rays amongst terrestrial sources. Beam divergence and size can therefore be minimized while retaining high flux, and for third-generation synchrotrons the coherence and phase of these sources can be investigated. These properties make synchrotrons ideal testing grounds for structural investigations using conventional crystallography, XAFS (x-ray absorption fine structure), DAFS (diffraction anomalous fine structure), MAD (multiple-wavelength anomalous dispersion) and other innovative approaches.

The complex temporal variation of the incident x-ray flux is often a major limiting factor in experiments, particularly at synchrotrons. Variation is due to rapid cycling of trapped electrons or positrons in the ring, at microsecond and nanosecond time-scales corresponding to beam revolution and bunch separations.¹ This rapid cycling is only observed in direct investigations of coherence (I. Mc Nulty, personal communication, 1999)² or picosecond time-dependent diffraction studies.^{3,4} Variation is due to the finite lifetime of the beam current, usually between 1 to 60 h. This lifetime decay varies from one day to the next but is stable over several minutes and is

easily corrected for by direct observation before and after a scan.

Further variation is due to noise in the x-ray flux with a time-scale of seconds or minutes, well above that expected from statistical considerations. For example, a monochromated undulator flux may be 10^{16} photons s^{-1} , whereas a corresponding bending magnet line flux may be 10^{12} photons s^{-1} for 5–15 keV x-ray energies. The statistical variation for 1 s should be 10^6 in the weaker case, or a relative variation of flux between observations of 10^{-6} . A beam lifetime of 20 h would result in a decrease in flux by 1.3×10^{-5} over the 1 s interval. The beam decay should therefore dominate over the statistical fluctuation. However, the observed flux variation in beamlines is much greater than 10^{-6} , and reaches 1%.

This additional noise arises from beam tuning operations, sudden losses (or fills) of the ring, physical drift in the beam position relative to a collimator, angular or divergence drift at monochromators and thermal effects on the primary or secondary monochromator crystals. One must therefore normalize experimental observations to incident flux as measured by a monitor counter. The method for matching detector characteristics is crucial, and understanding the nature of the noise is essential for optimizing final results. We compare the flux variation with detailed analysis of noise contributions in the experimental chain and point out valid and inappropriate methods for normalization. We illustrate the final limiting precision of such methods, and the new phenomena accessible with optimized investigations.

* Correspondence to: C. T. Chantler, School of Physics, University of Melbourne, Parkville, Victoria 3010, Australia.
Contract/grant sponsor: Australian Synchrotron Research Program.

The flux from a synchrotron beam is conventionally considered to have a symmetric Gaussian distribution with a simple decay trend, with identical mode and mean. Experimental arrangements allow the investigation of these assumptions. The nature of the statistical distribution is linked to the optimized analytical method. We directly investigate the nature of the statistical noise correlation between the two detectors, and measure the correlation of noise between the upstream and downstream detector signals. The correlation dictates the method of analysis and identifies contributions to the experimental statistics.

This paper discusses an incident flux passing through (Kapton) windows with negligible absorption into a monitor ion chamber detector. The flux is partially absorbed by the ion chamber gas, providing a normalization signal. An 'experimental sample' downstream is followed by a second matched ion chamber with the same gas flow. Hence we use ion chambers for normalization and investigating the experimental statistics. The discussion will be specific for matched ion chambers, but conclusions do not depend upon the detector type—similar results may be obtained with scintillators, PIN diodes and other detectors (these detectors are used in current mode, and minimize the statistical uncertainty due to the electron–ion currents as indicated in Table 2, but these fluctuations are dominated by the photon noise).

Previous recent studies have addressed elements of this problem in relation to specific XAFS experiments.⁶ Their concerns do not address the issues presented here (such studies do not sample wide ranges of energies, multiple fluxes or multiple log ratios, and so are unable to isolate dependences upon time or contributions dominating only in particular regimes of flux and energy). We have previously discussed ion chamber ionization and detection processes at synchrotrons,⁷ and the response function of image plates.⁸ These studies are relevant to this paper, but concepts discussed in those studies will not be repeated;

we will discuss more general issues and tools for improving experimental methods.

CHARACTERIZATION OF DETECTORS

In the high-flux beam of a synchrotron, ion chambers are widely used because they can have low absorption and can cope with high fluxes without saturation. The linearity of ion chambers is often unsatisfactory across an energy range of a factor of 2–3. Saturation and arcing occur in very high-flux situations on undulator ID lines at the latest synchrotrons such as APS (J. Wang, A. Stampfl and I. McNulty, SRICAT, APS, Chicago, personal communication) and also at NSLS.⁷

Ideal monitor absorption of 10% may be designed by a mix of gases for a given energy but will be non-ideal at energies differing by only 1 keV. Hence investigations covering wide energy ranges must change gas mixtures or allow for the changing monitor efficiency. For an investigation below 7 keV, pure nitrogen flow ion chambers at ambient pressure (200 mm in length) yield an optimum balance between efficiency and attenuation (Fig. 1). Maximizing absorption in the downstream detector is crucial to avoid seriously compromising the statistical precision. Decreasing the active detection length of the upstream monitor significantly improves the lower energy limit, but has a marginal effect on medium-energy performance. Above 13 keV, pure argon flow ion chambers offer the best balance, so a gas mixture is only useful between 7 and 13 keV. Below 5–7 keV, any argon mixture is too strongly attenuating by orders of magnitude. We investigate photon energies from 5 to 20 keV and therefore use nitrogen-filled ion chambers, with brief reference to equivalent performance for a 24:76 argon–nitrogen mixture.

Ion chamber linearity depends upon the detector geometry, beam size and alignment, the gas, and the amplifiers.

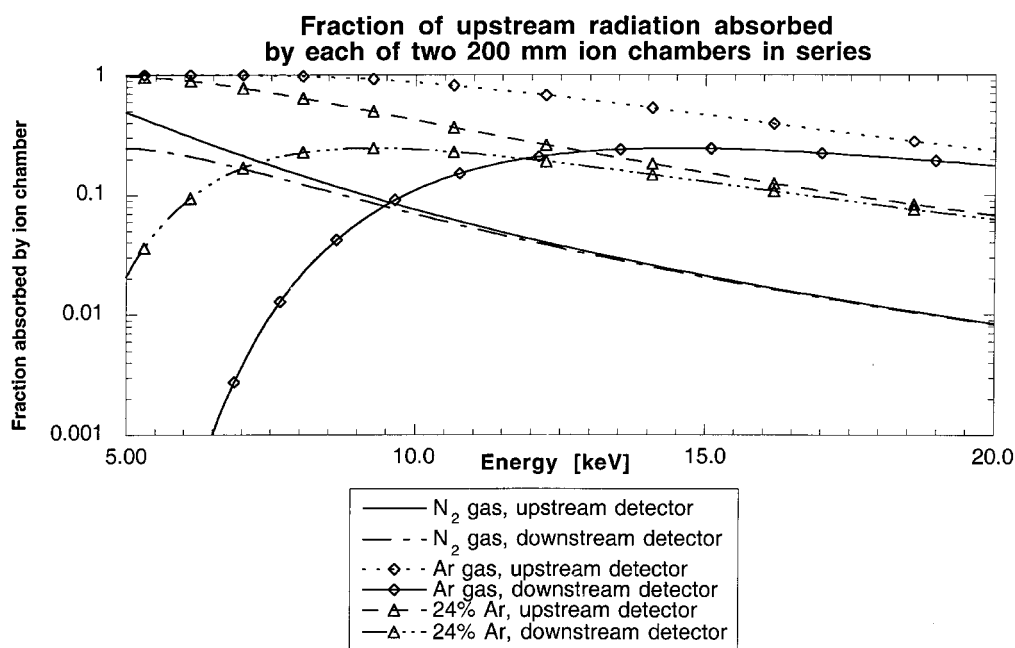


Figure 1. Fraction of upstream radiation absorbed by ion chamber composition (Ar–N₂ mixtures) as a function of energy, for specific paired ion chambers in series. Counting rates drop by three or more orders of magnitude if not appropriately optimized.

Statistical precision is optimized by increasing the flux and decreasing the amplification. This may also optimize the detector linearity by avoiding saturation and background noise. A flux below the saturation limit, amplified to give a reading near the counting limit, has the greatest number of significant figures. The last few digits may be inaccurate and non-linear. The 10^{10} amplification scale of the Keithley amplifier used in this study was unstable with high noise levels; lower scales (10^9 and 10^8) were orders of magnitude more stable. Hence a lower amplification factor with sufficient flux will optimize precision and linearity and additionally minimize amplifier noise.

Ion chambers yield a current, amplified and converted to a voltage as a 'count-rate.' It is sometimes stated that they cannot have photon-counting statistics. This conclusion is false—every component of a detector chain adds to the total noise and the total statistics. The statistical variation in the incoming flux contributes directly to the total statistical variation of the detected flux. The smaller number of photons actually absorbed generates a correspondingly larger statistical variation.

We pass over details of x-ray fluorescence processes where photons are re-emitted, and of the inverse process (capture of a photoelectron by an ionized atom to release another x-ray—rare except at saturation).⁷ We neglect mechanisms for loss of conversion efficiency to electron-ion pairs and therefore assume a reliable effective energy per electron-ion pair (e.g. 27.2 ± 1.8 eV for argon). Hence the detected current will have a simple distribution and statistics from that of the absorbed number of photons.

The amplifier and analogue-to-digital converter contribute electronic noise with several components, leading finally to the 'count-rate' observed. Offsets of electronic bias are added to the detected signal before amplification. With incorrect electronic offsets or faulty power supplies, these electronic bias contributions dominate over other error sources. The relative contribution from timing errors is $<10^{-6}$ for counting periods >1 s.

Readers with experience in experimental work will find comments regarding saturation and offsets to be elementary. However, at what level do these various contributions dominate, and how can this be optimized? Our estimates are quantified for an experiment at the Australian National Beamline Facility in Tsukuba, Japan, in Table 1, which also specifies symbols for the different flux measures. We differentiate between the photon flux after monochromation I_{up} , the flux of photons absorbed

per second in the upstream monitor I_{absup} or downstream detector I_{absdown} and the integrated current readings of detectors I_{M} and I_{D} .

CORRELATION OF THE DETECTORS

Assuming uncorrelated and Gaussian variation in the two detectors, we have the usual relation for the standard deviation of the normalized signal $I_{\text{D}}/I_{\text{M}}$, where I_{D} is the value recorded in the downstream detector, I_{M} is the upstream monitor signal and σ_{D} and σ_{M} are the corresponding standard deviations:

$$\left[\frac{\sigma_{(I_{\text{D}}/I_{\text{M}})}}{I_{\text{D}}/I_{\text{M}}} \right]^2 = \left(\frac{\sigma_{\text{D}}}{I_{\text{D}}} \right)^2 + \left(\frac{\sigma_{\text{M}}}{I_{\text{M}}} \right)^2 \quad (1)$$

Each relative detector uncertainty ($\sigma_{\text{D}}/I_{\text{D}}$ and $\sigma_{\text{M}}/I_{\text{M}}$) then involves the quadrature sum of all contributing uncorrelated relative fluctuations. However, the detector and monitor signals are correlated, with a correlation coefficient R . For $R = 1$, Eqn (1) is modified to

$$\left[\frac{\sigma_{(I_{\text{D}}/I_{\text{M}})}}{I_{\text{D}}/I_{\text{M}}} \right]^2 = \left| \left(\frac{\sigma_{\text{D}}}{I_{\text{D}}} \right) - \left(\frac{\sigma_{\text{M}}}{I_{\text{M}}} \right) \right|^2 \quad (2)$$

If both signals increased by +10% between measurements, then there is no error in the ratio due to this variation. Similarly, a correlation between detector signals of $R = -1$ leads to

$$\left[\frac{\sigma_{(I_{\text{D}}/I_{\text{M}})}}{I_{\text{D}}/I_{\text{M}}} \right]^2 = \left| \left(\frac{\sigma_{\text{D}}}{I_{\text{D}}} \right) + \left(\frac{\sigma_{\text{M}}}{I_{\text{M}}} \right) \right|^2 \quad (3)$$

Table 2 is unique in isolating eight contributions to the total fluctuations and predicting their magnitudes for a typical run at ANBF using the data in Table 1. Some contributions are statistical, and behave as expected for synchrotrons, but some are not Gaussian and behave differently. Some follow Eqn (1) and are uncorrelated, whereas others follow Eqn (2) or (3), requiring a different analysis.

The beamline includes all contributions, and the optimum data collection and analysis minimize some of these components. Many experiments perform fairly well without this optimization. Key issues may be addressed in similar ways to those discussed here, but more commonly

Table 1. Fluxes for a typical bending magnet beamline

Parameter	Symbol	5 keV	10 keV	20 keV
Synchrotron output flux [photons s^{-1} (0.1% bandwidth) ⁻¹]		10^{11}	10^{11}	10^{10}
ANBF estimated beamline flux after monochromation	I_{up} (c.p.s.)	10^9	10^9	10^8
Percentage attenuation inside 200 mm N_2 ion chamber, 1 atm	A_{ion} (%)	50	7.6	0.8
Photons absorbed per second by upstream ion chamber	I_{absup}	2.5×10^8	7.6×10^7	8×10^5
Photons absorbed per second by downstream ion chamber	I_{absdown}	2.5×10^8	7.0×10^7	8×10^5

Table 2. Predicted fluctuations (1 s.d., $\sigma_{\text{rel}} = \sigma_{\text{abs}}/I$) from various sources, based on the assumptions in Table 1 and in the text

Parameter	s.d./ I , σ_{rel}	Energy 5 keV	Energy 10 keV	Energy 20 keV	R : anticipated correlation coefficient between detectors	Reduction of s.d./ I for 100 s counting time, relative to 1 s counting
Statistical contribution from incident flux on upstream monitor (1 s count)	σ_{up}	3.2×10^{-5}	3.2×10^{-5}	10^{-4}	1	$\times 10^{-1}$
Statistical contribution from absorbed flux on upstream monitor and effect on downstream detector	σ_{absup} ; σ_{updown}	4.5×10^{-5} ; 4.5×10^{-5}	1.1×10^{-4} ; 9.5×10^{-6}	1.1×10^{-3} ; 9.5×10^{-6}	-1	$\times 10^{-1}$
Statistical contribution from absorbed flux on downstream detector	σ_{absdown}	6.3×10^{-5}	1.2×10^{-4}	1.1×10^{-3}	0	$\times 10^{-1}$
Additional fluctuation of electron-ion currents (~ 16 eV per ion pair)	σ_{ionup}	4×10^{-6}	4.8×10^{-6}	3.1×10^{-5}	0	$\times 10^{-1}$
Timing error (10 μ s estimated)	σ_{time}	10^{-5}	10^{-5}	10^{-5}	1 (single pulse); 0 (counters not synchronized)	$\times 10^{-2}$
Decay of flux from current lifetime (10 h lifetime assumed)	σ_{decay}	2.6×10^{-5}	2.6×10^{-5}	2.6×10^{-5}	1	$\times 10^2$
Amplifier and conversion noise?	σ_{amp}	10^{-6}	10^{-6}	10^{-6}	0, ± 1 ?	$\times 1$

experiments may not be fully optimized, in which case error bars may be poorly determined. This a primary concern of this paper.

In Table 1, we assume the photons incident on the upstream monitor are attenuated only by the gas inside the monitor before reaching the downstream detector. The air gap, window thickness and the attenuator for the experiment are neglected for simplicity in Table 2. In attenuation measurements I_{absup} and I_{absdown} , or I_{M} and I_{D} , are often given as I_0 and I . We distinguish parameters to emphasize the use of measured parameters to determine theoretical contributions to statistical noise. *Observed* standard deviations in photons are given as σ_{D} and σ_{M} , for comparison with the literature. *Predicted* fluctuations in Table 2 are given as relative standard deviations $\sigma_{\text{rel}} = \sigma_{\text{abs}}/I$ to simplify equations.

Table 2 indicates the expected correlation between monitor and detector signals as a function of the type of fluctuation. The incident beam-flux noise should have a correlation coefficient of unity between ion chambers as both see the same percentage change in flux. Additional noise due to electron-ion pair numbers is uncorrelated as the charge amplification in one ion chamber should be independent of that in the other. Amplifier and conversion noise can be complex, uncorrelated or correlated by power supply faults.

The second row in Table 2 has a negative R : if the upstream monitor absorbs an extra 1% of the incident flux (due to some statistical variation) then the downstream detector receives less flux (1% of the upstream flux or say 2% of the downstream flux, if the monitor absorbs 50% of the incident flux). This statistical contribution will therefore have $R = -1$ between variations in the upstream and downstream signals. The positively correlated noise (incident beam-flux) may be dominated by

this anti-correlated component. However, the slope of the correlated component is unity (an increase of 1% incident flux upstream yields a 1% increase of incident flux downstream) while the anti-correlated component has a slope given by $f_1/(1 - f_1)$, where f_1 is the attenuation fraction inside the monitor. Hence, except at low energies where f_1 exceeds 50%, the correlated component dominates.

A comparison of statistics of paired detectors over different counting periods should identify the dominant contributions to the final statistics, without unnecessary or invalid assumptions. Any investigation of statistics and noise requires multiple sampling and repeated measurements, to define R . Otherwise there can be no informed analysis of the results. Isolated measurements may yield strong accidental correlations between causally uncorrelated components, but this accidental correlation should be randomly distributed.

The last column of Table 2 indicates whether the relative contributions from these components will vary with observations over different time-scales. Any (normal) statistical counting contribution will decrease as $1/\sqrt{N}$. The timing error is presumed to be of constant magnitude, so a longer counting period will reduce this relative error. The beam-current decays roughly linearly with time (exponentially with a small coefficient). The amplifier and conversion noise will depend upon gain and offset, and may result in a constant error or contain a statistical component.

EFFECT OF CORRELATION ON THE OPTIMUM METHOD OF ANALYSIS

If the correlation coefficient between the monitor and detector signals in a data series is $R = -1$, the variation

of I_D/I_M is much greater than the variation of either I_D or I_M , so much so that the correct parameter to report is the ratio of the means rather than the mean of the ratios, with a considerably reduced variance:

$$\left[\frac{\sigma_{(\overline{I_D/I_M})}}{\overline{I_D/I_M}} \right]^2 = \left| \left(\frac{\sigma_{I_D}}{I_D} \right) - \left(\frac{\sigma_{I_M}}{I_M} \right) \right|^2 \quad (4)$$

For a correlation coefficient R , the mean of the ratios has an associated variance of

$$\left[\frac{\sigma_{(\overline{I_D/I_M})}}{\overline{I_D/I_M}} \right]^2 = \left(\frac{\sigma_D}{I_D} \right)^2 + \left(\frac{\sigma_M}{I_M} \right)^2 - 2R \left(\frac{\sigma_D}{I_D} \right) \left(\frac{\sigma_M}{I_M} \right) \quad (5)$$

while the ratio of the means has an associated variance of

$$\left[\frac{\sigma_{(\overline{I_D/I_M})}}{\overline{I_D/I_M}} \right]^2 = \left(\frac{\sigma_D}{I_D} \right)^2 + \left(\frac{\sigma_M}{I_M} \right)^2 + 2R \left(\frac{\sigma_D}{I_D} \right) \left(\frac{\sigma_M}{I_M} \right) \quad (6)$$

For positive R the mean of the ratios should be reported, whereas for negative R the ratio of the means should be given. This optimizes the use of beam time and the precision of final results.

ELECTRONIC OFFSETS

Electronic bias offsets lead to observed signals $I_{M,off}$ and $I_{D,off}$ in the absence of any photon flux. The corresponding noise dominates for low counts and poor statistics, e.g. when using a very thick attenuator. Bias offsets should be measured with the primary measurement. Analogues of Eqns (1) and (5) are

$$\left\{ \frac{\sigma_{[(I_D - I_{D,off})/(I_M - I_{M,off})]}}{(I_D - I_{D,off})/(I_M - I_{M,off})} \right\}^2 = \frac{\sigma_D^2 + \sigma_{D,off}^2}{(I_D - I_{D,off})^2} + \frac{\sigma_M^2 + \sigma_{M,off}^2}{(I_M - I_{M,off})^2} \quad (7)$$

$$\left\{ \frac{\sigma_{[(I_D - I_{D,off})/(I_M - I_{M,off})]}}{(I_D - I_{D,off})/(I_M - I_{M,off})} \right\}^2 = \frac{\sigma_D^2 + \sigma_{D,off}^2}{(I_D - I_{D,off})^2} + \frac{\sigma_M^2 + \sigma_{M,off}^2}{(I_M - I_{M,off})^2} - 2R \left[\frac{\sqrt{\sigma_D^2 + \sigma_{D,off}^2}}{(I_D - I_{D,off})} \right] \left[\frac{\sqrt{\sigma_M^2 + \sigma_{M,off}^2}}{(I_M - I_{M,off})} \right] \quad (8)$$

If I_D and I_M are positively correlated, we should use Eqn (8). Inappropriate use of these equations will increase variance and corresponding errors in results. However, to apply Eqn (7) or (8) reliably requires avoiding drifts in the offset level and determining the electronic offsets to high accuracy.

EXPERIMENTAL EXAMPLES AND DISCUSSION

These theoretical predictions are accurate, but do they have practical application? Can component fluctuations be measured and identified? We illustrate these issues for

simple cases with observed data, and discuss this in the context of an x-ray attenuation study, following Chantler *et al.*⁹ The methods are independent of the nature of the measurement or detectors. All x-ray measurements involve scattering or absorption, so the net benefit is similar for crystallographic and XAFS determinations. Many crystallographic determinations do not require high relative precision of intensities or absolute structure factors to determine atomic species, lattice groups or atomic locations to moderate accuracy. However, accurate determination of temperature factors, bonding, electron density studies and structural determinations or organometallic molecules all benefit from increased precision.

DO CONSECUTIVE MEASUREMENTS HAVE COMMON MEANS (I_D AND I_M), STANDARD DEVIATIONS (σ_M) AND NOISE DISTRIBUTIONS? WHAT IS THE TIMING ERROR (σ_{TIME})? ARE FLUCTUATIONS NORMALLY DISTRIBUTED?

Two consecutive scans of data were taken with the ANBF monochromator set to 20 keV, with each measurement taking 3 s. The observed monitor (upstream) percentage standard deviations (% s.d.s) for each of the two 21-point (i.e. 21-measurement) distributions was $\sigma_M/I_M = 1.28 \times 10^{-3}$ and 9×10^{-4} , versus the prediction from Table 2 of $\sigma_M/I_M = 1.1 \times 10^{-3}/\sqrt{3} = 6.4 \times 10^{-4}$. The two scans are consecutive but are disjoint, i.e. they do not have a common mean. Any trend over each scan of $21 \times 3 = 63$ s is dominated by noise (short-term beam fluctuation). In all cases, the timing readout is accurate to $\delta_{time}/I_M = 10^{-5}$ and consistent with a systematic error of $\sigma_{time}/I_M = 0.5 \times 10^{-5}$.

The two % s.d.s differ by 40%. The probability of a normal population s.d. >1.1 times the sample s.d., or <0.8 × s.d. (sample) is about 10%.¹⁰ The normal probability of s.d. (pop) = s.d. (sample) × 1.4 is 0.5%, and the normal probability of s.d. (pop) = s.d. (sample)/1.4 is still only 3.2%.¹¹

The two results could have the same population s.d., but this is unlikely (3%) if normal distributions are assumed.^{10,11} Hence the % s.d.s appear disjoint. Further observed distributions suggest that the distribution is *not* normal, but that the source of variation is consistent between measurements. This appears true for most beam-lines.

DO PREDICTIONS OF NOISE AGREE WITH OBSERVED STANDARD DEVIATIONS (σ_M , σ_D)?

A typical series of independent data for 20 keV is given in Table 3 for five different attenuator samples, together with a 'zero offset' (i.e. beam off) test. The downstream (detector) results are disjoint for all attenuators, since they involve different thickness and attenuation. (The second and fourth rows are measurements with no attenuator, and are conjoint for the downstream detector statistics.) Each group is of 10 points (10 measurements) of 1 s each. Any trend is dominated by short-term variation.

The range of observed upstream % s.d.s is again 40% so all distributions may again have the same population

Table 3. Observed fluctuations for five independent groups of data, each composed of 10 repeated measurements of 1 s duration, compared with predictions based on Table 2

Summary table: different targets: monitor (upstream) results				Predicted: Table 2, with no offset correction				Detector (downstream) results				Predicted: Table 2, with no offset correction		With zero offset [Eqn (8)]
Monitor mean I_M	s.d.	s.d./ I_M $\times 10^3$	s.e./ I_M $\times 10^3$	s.d./ I_M $\times 10^3$	Observed/ predicted	Detector mean I_D	s.d.	s.d./ I_D $\times 10^3$	s.e./ I_D $\times 10^3$	s.d./ I_D $\times 10^3$	Observed/ predicted	s.d./ I_D $\times 10^3$		
35320.6	51.90	1.47	0.465	1.10	1.34	5504.2	8.01	1.46	0.460	2.73	0.53	2.93		
34816.5	36.73	1.05	0.334	1.10	0.96	33874.3	43.72	1.29	0.408	1.10	1.17	1.10		
34682.6	37.60	1.08	0.343	1.10	0.99	1551.7	2.87	1.85	0.585	5.12	0.36	7.52		
34583.9	36.35	1.05	0.332	1.10	0.96	33664.4	40.47	1.20	0.380	1.10	1.09	1.10		
34513	51.93	1.50	0.476	1.10	1.37	20268.9	35.45	1.75	0.553	1.42	1.23	1.43		

s.d. Irrespective of the nature of the distribution, this consistency suggests that the distributions are the same. Predictions based on Tables 1 and 2, in Table 3, show that the ratio of observed/predicted variation is about 1.0 for monitor signals, and perhaps the same for the detector distributions. Hence the predicted number of photons incident on the detectors, and the number of photons absorbed by the detectors, appear accurate to within a small factor.

We report the relative or percentage s.d.s of a single measurement, σ_M/I_M , and the corresponding relative standard error of the scan of measurements $s.e./I = \sigma_M/(I_M\sqrt{N})$. The standard error gives the best estimate of the combined measurement precision, and in the absence of any trend or discontinuity, will improve with counting time as $1/\sqrt{N}$.

ON WHAT TIME-SCALE IS A TREND DOMINANT? NON-NORMALLY DISTRIBUTED OUTLIERS AND CONSISTENCY OF TRENDS IN FLUX (σ_{DECAY})

Another series of 20 keV data (Table 4) is identical with that in the previous section but with a significantly longer time-scale. Any trend *within* each group over $10 \times 5 = 50$ s is still dominated by short-term noise. The time elapsed between measurements varies from 52 s (Nos 1 and 2) to 136 s (Nos 4 and 5). The upstream means are significantly different. Here, the approximately linear trend in time *between* groups in the series dominates over the short-term noise.

Often means are inconsistent owing to a trend in the data, as with the beam decay in this example. The relative s.d.s may still be consistent, indicating a common source of noise. Then a pooled result will be superior to individual measurements. It is also possible that means are consistent but the source of noise varies, leading to inconsistent % s.d.s in independent scans of data.

In Table 4, observed upstream s.d.s vary by a factor of two. The probability of s.d. (pop) = s.d. (sample) $\times 1.4$ is only 3%, whereas the probability of s.d. (pop) = s.d. (sample)/1.4 is 13% assuming normal distributions. Hence the extreme s.d.s in the monitor measurements appear disjoint. The probabilities depend on the number of sampled points.

The dominant outlier (scan No. 3, s.d. = 308) is dominated by a single outlying point, removal of which leads to an s.d. (190) and a mean (230 506) consistent with the following scan (No. 4). Hence a non-normally distributed outlier impaired the comparison and should be removed. If the outlier is removed the range of s.d.s is only 50% and all distributions could be consistent with a common s.d. of 175. Irrespective of the nature of the distribution, this again implies that the distributions are the same.

The ratio of observed/predicted variation in Table 4 is 1.5–1.6 for monitor signals and perhaps 1.4 for detector distributions, suggesting that the photon flux (if dominant) was overestimated by a factor of two. The detector signals are disjoint since the sample attenuator is different for different data scans.

An even longer time-scale is given in Table 5 with a series of 10 groups of data. Each downstream measurement

Table 4. Observed fluctuations for five independent groups of data, each composed of 10 repeated measurements of 5 s duration, compared with predictions based on Table 2

Summary table: different targets: monitor (upstream) results				Predicted: Table 2 absorbed flux, no decay contribution no zero offset				Detector (downstream) results				Predicted: Table 2, with no offset correction		Predicted: With zero offset [Eqn (8)]
Monitor mean I_M	s.d.	s.d./ I_M $\times 10^4$	s.e./ I_M $\times 10^4$	s.d./ I_M $\times 10^4$	Observed/ predicted	Detector mean I_D	s.d.	s.d./ I_D $\times 10^4$	s.e./ I_D $\times 10^4$	s.d./ I_D $\times 10^4$	Observed/ predicted	s.d./ I_D $\times 10^4$		
229383	136.59	5.95	1.88	4.92	1.21	128834	88.48	6.87	2.17	6.46	1.06	6.51		
229398	150.72	6.57	2.08	4.92	1.34	222357	132.26	5.95	1.88	4.92	1.21	4.92		
230586	308.68	13.4	4.23	4.92	2.72	16786	22.34	13.3	4.21	17.9	0.74	20.6		
230496	210.23	9.12	2.88	4.92	1.85	223372	214.26	9.59	3.03	4.92	1.95	4.92		
232254	193.77	8.34	2.64	4.92	1.70	147524	127.50	8.64	2.73	6.05	1.43	6.08		
1781	3.77	21.2	6.70			4250	2.26	5.32	1.68					

^a Predictions with zero offset corrections in this case are poor because the zero offset measurement was relatively poor and the trend in the data is not properly evaluated. This is corrected by longer observations as presented in Tables 5 and 6 and discussed in the text.

Table 5. Observed fluctuations of the upstream monitor for 10 independent groups of data, each composed of 11 repeated measurements of 20 s duration, after removal of linear trend, compared with predictions based on Table 2

Row No. (data scan)	Summary table: mesh measurement: monitor measurements				Predicted: Table 2, absorbed flux, no decay contribution, no zero offset		Average slope in time series	Decay contribution: linear estimate	Predicted: with decay contribution, no zero offset
	Monitor mean I_M	s.d.	s.d./ $I_M \times 10^4$	s.d./ $I_M \times 10^4$	s.d./ $I_M \times 10^4$	Observed/predicted	$\sigma_{\text{decay}} \times 20$ s Decay per 20 s	s.d./ $I_M \times 10^4 = \sigma_{\text{decay}} (1 \text{ s}) \times 2 \times 10^5$	Observed/predicted
-4	559172	155.489	2.78	0.838	2.46	1.13	-87.8364	1.57	0.95
-3	558313	280.38	5.02	1.51	2.46	2.04	-55.80	0.999	1.89
-2	557531	369.649	6.63	2.00	2.46	2.70	-114.75	2.06	2.07
-1	556771	298.562	5.36	1.62	2.46	2.18	-70.01	1.26	1.94
0	555846	203.052	3.65	1.10	2.46	1.49	-68.05	1.22	1.33
1	554669	262.594	4.73	1.43	2.46	1.92	-128.75	2.32	1.40
2	553788	236.821	4.28	1.29	2.46	1.74	-58.03	1.05	1.60
3c	892133	1518.08	17.00	5.13	2.46	6.92	-696.10	7.80	2.08
4	896156	697.148	7.78	2.35	2.46	3.16	763.96	-8.52	0.88
3a	552816	327.336	5.92	3.42	2.46	2.41	-183.50	3.32	1.43

has a (slightly) different sample thickness and attenuation, and so may be disjoint. We call this set of data a mesh measurement, as the measurements map a rectangular grid of the thickness variation across the attenuator. Upstream groups appear disjoint. For each $11 \times 20 = 220$ s interval, the noise is dominated by the trend. In this extreme case, the beam dumped in the middle of the set of measurements. Individual groups show large decay and fill cycles and trends are clear over 40–60 s.

Fitting a slope isolates the average decay rate from the symmetric fluctuations. The upstream trend represents a decay ratio per second (σ_{decay}) from 5×10^{-6} to 11×10^{-6} , or from 37×10^{-6} to -41×10^{-6} for the dump/fill sections. These trends are consistent for upstream and downstream signals, with the attenuated downstream signal corresponding to an s.d. of $\sigma_{\text{decay}} \approx 5 \times 10^{-6}$.

The decay indicates a lifetime from 2.5 to 5 h (neglecting the dump/fill sections), rather than the estimate of 10 h in Table 2 based on reported beamline lifetimes. This result is reasonable, and emphasizes the utility of quantitative monitoring of beam fluctuations during precision measurements.

In other words, this analysis provides a direct measure of the beam performance independently of any displayed beam current profile provided by the synchrotron operators. This observed trend in delivered flux is of direct relevance to the experiment since the beam current would be

affected by tracking of the beam across a monochromator or collimating slit.

Removing the linear trend yields reduces s.d.s by a factor of 3 and leads to close agreement between predicted and observed % s.d.s. We obtain the monitor (upstream of an absorber) summary in Table 5 and the detector (downstream) summary in Table 6. For the upstream data, the s.d.s vary by a factor of 5, even relative to the changing means after refilling. The probability of a normal population s.d. = s.d. (sample) $\times 1.4$ is only 3%, whereas the probability of s.d. (pop) = s.d. (sample)/1.4 is 11%. Although the linear trend is removed, the fluctuations from the rate of change of data (decay or refill) between adjacent points are of the same magnitude. The variation between the beginning and end of a single 20 s data point is a significant contribution to the overall variation. Taking this into account yields results consistent with a common ratio of observed/predicted variation of about 1.4–1.6 for monitor signals, suggesting that the absorbed photon flux is half that predicted in Table 2. This is consistent with the reduction of flux between tests by about a factor of two, due to the decay of the beam. The means and s.d.s are disjoint but the basis for the variation is understood.

The attenuated detector signal has a larger relative variance than the monitor signal, as expected. The increased relative uncertainty due to photon counting dominates over corrections involving the zero offset and decay

Table 6. As for Table 5, but for the downstream detector

Summary table: mesh measurement: detector results				Predicted: no decay contribution, no zero offset		Predicted: no decay contribution, but with zero offset [Eqn (8)]		Predicted: with decay contribution, and zero offset	
Detector mean I_D	s.d.	s.d./ $I_D \times 10^3$	s.e./ $I_D \times 10^3$	s.d./ $I_D \times 10^3$	Observed/predicted	s.d./ $I_D \times 10^3$	Observed/predicted	Observed/predicted	Observed/predicted
48932.9	144.32	2.95	8.89	8.31	3.55	1.01	2.91	2.88	
48455.5	154.31	3.18	9.60	8.35	3.81	1.02	3.12	3.11	
47789.4	93.17	1.95	5.88	8.40	2.32	1.03	1.89	1.85	
47218.6	99.60	2.11	6.36	8.45	2.50	1.04	2.03	2.01	
46834.1	123.75	2.64	7.97	8.47	3.12	1.05	2.53	2.51	
46746.6	128.19	2.74	8.27	8.47	3.24	1.05	2.62	2.56	
46967.6	87.98	1.87	5.65	8.45	2.22	1.04	1.80	1.79	
65591.7	151.23	2.31	6.95	9.07	2.54	1.04	2.21	1.77	
66197.3	155.61	2.35	7.09	9.05	2.60	1.04	2.26	1.75	
47023	35.59	0.757	2.28	8.43	0.90	1.04	0.73	0.69	

variability during the 20 s measurement. The ratio of observed/predicted % s.d.s $[(\sigma_D/I_D)_{\text{observed}}/(\sigma_D/I_D)_{\text{predicted}}]$ is nearly 2, significantly larger than monitor results $[(\sigma_M/I_M)_{\text{observed}}/(\sigma_M/I_M)_{\text{predicted}}]$. This enhancement arises from using sequential measurements of significantly (1%) different thicknesses of attenuator. These variations (between points) dominate over the statistical variation and trends. Hence we are measuring thickness variations to better than 1%.

WHAT PRECISION DO THESE RESULTS IMPLY?

We refer to the data set presented in Tables 5 and 6 (the mesh measurement), and to a second mesh measurement of similar quality for a different attenuator sample.

Pooled variances

The variations in attenuation across the sample meshes are 2.2 and 7.6%, respectively. This pooled variance σ_P^2 [Eqn (1)] gives $\sigma_P(I_D/I_M)/(I_D/I_M) = 1\%$ or 3% precision, and suggests that relative attenuation may be determined to 1%. This precision is for a random location on the attenuator, and is much larger than for a well-defined location at a specific point of the mesh. Many literature measurements of attenuation are limited at the 1–3% level, for this reason.¹²

Uncorrelated signals

The reproducibility at a fixed location must be determined by additional experiments. The upstream monitor and downstream detector variances, following the procedure used for Tables 3 and 4, yield s.d.s of 0.5 and 0.22%, respectively. These estimates assume uncorrelated signals, following Eqn (7). This estimate [Eqn (7)] describes a quadrature sum of the noise in both detectors, which can be appropriate in some experiments. However, we predict significant noise components with both positive and negative correlation. The positive correlation dominates in the optimized work described here, and this uncorrelated estimate of limiting noise is also poor.

Correlated signals

A correct estimate of reproducibility for correlated signals (between upstream and downstream detectors) is given by Eqn (8). Approaching this limit requires the determination of R for each pair of upstream and downstream data scans, in each experimental arrangement. The actual % s.d.s resulting from this approach yield precisions of 0.15 and 0.045% for these two data sets. This precision is confirmed by the reproducibility of the extracted ratio from individual paired I_M and I_D measurements, i.e. from the % s.d.s of the $j = 1$ to N measurements of the point-to-point ratio

$$[(I_D - I_{D,\text{off}})/(I_M - I_{M,\text{off}})]_j \quad (9)$$

Allowance for all correlation [Eqn (8) or (9)] is the optimal approach, and the net increase in precision observed by factors of 7 or 70, respectively, is dramatic. The difference between the two results obtained (0.15 and 0.045%) can also be optimized by sample preparation, selection and data collection, so that an optimized figure of 0.05% for the limiting sample s.d. is achievable in many cases.

Standard errors

The correct reported uncertainty on the mean is the standard error of the ratio, a factor of 3–5 smaller for 10–21 data points per measurement. Hence the nominal statistical quality of the determined ratio should approach a relative standard error s.e. $(I_D/I_M)/(I_D/I_M) = 0.03\text{--}0.01\%$.

WHAT DO THE NOISE DISTRIBUTIONS LOOK LIKE?

To investigate the distribution of noise and not simply the point estimators (mean, s.d., kurtosis), we must collect long series of data on time-scales maximizing each noise component. A long time series at 20 keV composed of 19 groups of 11 measurements of 5 s per point (1045 s in total) is shown in Fig. 2. This exhibits the features observed earlier. The synchrotron decay trend and point deviations from it are clear, and so is a series of discontinuities and correlated excursions from the trend. The distribution is *not* normal because of the decay. In this relatively quiet set of data, the percentage decay is about $2 \times 10^{-5} \text{ s}^{-1}$, corresponding to a lifetime of 12 h. We can remove a linear or exponential trend fitted to the data. Then the pooled variance (the apparent s.d. of the total set) is much reduced, but the resulting distribution is still not normally distributed, as there are specific discontinuities whenever a significant beam loss or injection occurred. If these significant discontinuities are not removed from the data, the resulting noise distribution (the pattern of deviations from the mean) represents a square profile or top-hat distribution. After the trend and discontinuities are removed from the data, the data are similar to a normal distribution (Fig. 3). The width of the distribution matches that of a corresponding normal distribution (fit).

However, the distribution width and % s.d. is still significantly larger than would be predicted on the basis of the statistical noise fluctuations of the beam flux (Tables 5 and 6). In other words, there are three additional large contributions to computed s.d.s revealed by this investigation. Over medium or long time-scales the decay becomes dominant; the discontinuous loss (or gain) of flux in the beam can be dominant during short time-scales, and the normally distributed noise distribution is broader than that due to the estimated flux of photons entering the monitor detector, hence there is an additional normally distributed statistical source of noise.

CONCLUSIONS

The method presented allows the investigation of statistical components and correlation of contributions to fluctuations in an x-ray source. We have applied this to a typical

Time series of long term decay - upstream monitor, 20 keV

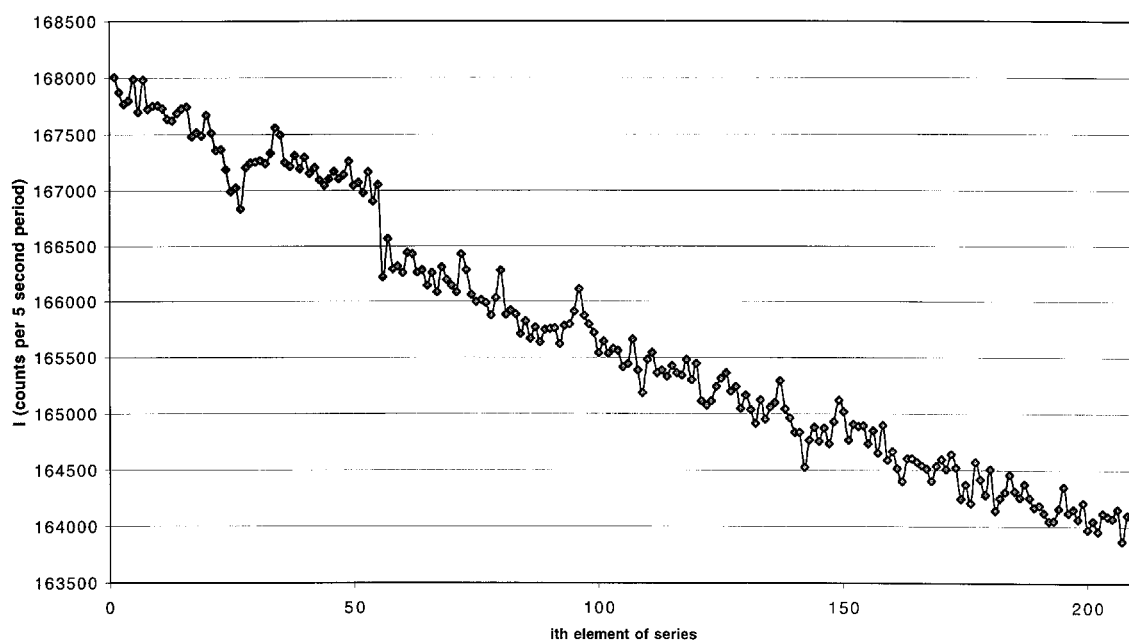


Figure 2. Time series of long-term monitor signal.

Observed Distribution compared to Normal Distribution after removal of discontinuity and linear decay trend

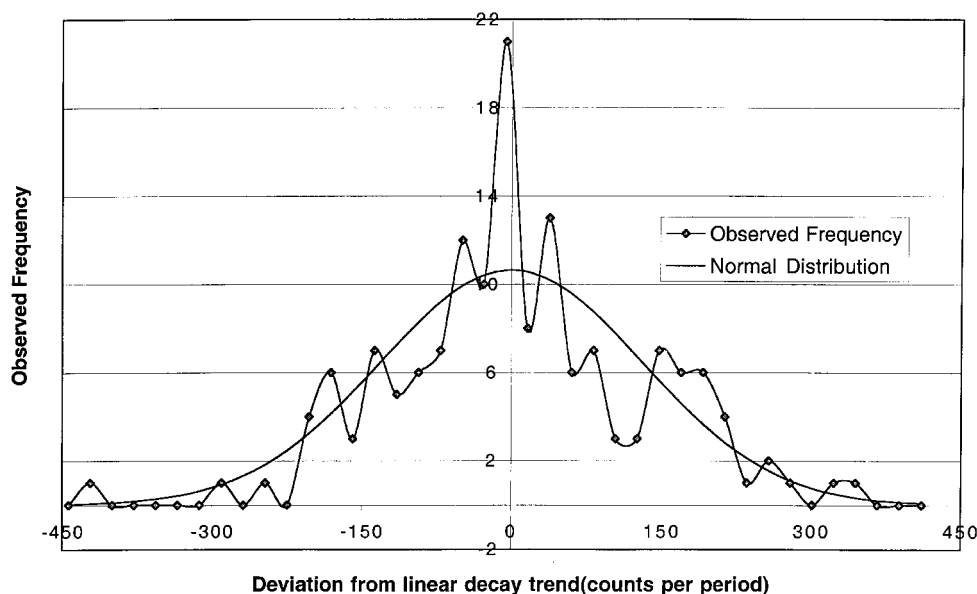


Figure 3. Observed distribution of noise after removal of linear trend and discontinuity.

bending magnet beamline using ion chamber detection. The fluctuations are not well predicted by using quoted synchrotron beam fluxes and beam current decay profiles, and they are not well predicted using a normal distribution plus a simple linear or exponential trend. Quoted fluxes can assess some component fluctuations to within a factor of two, but omit significant contributions to observed fluctuations.

The operator-provided beam current does not reflect discontinuities and fluctuations in the flux delivered to an experimental hutch, due for example to beam wandering

relative to the monochromating and collimating elements. The decay rate, level of discontinuities and additional symmetrically distributed noise can dominate over other sources of fluctuation on time-scales between seconds and hours.

Pooled relative standard deviations of $\sigma_P(I_D/I_M)/(I_D/I_M) = 1-3\%$ have limited precision in previous attenuation experiments. With appropriate optimization and analysis, this uncertainty is reduced to relative standard errors s.e. $(I_D/I_M)/(I_D/I_M) = 0.01-0.03\%$. This residual variance appears systematic in origin, and it may be

possible to improve this 0.01% precision further through a refinement of our approach.

Flux discontinuities and upstream positively correlated noise in excess of the photon statistics play a major role in the observed statistics, and predicate proposed routes of experimental set-up and analysis. This positively correlated upstream variation was the dominant noise additional to our predicted contributions. The trend of decay or filling of the beam current is not a simple or smooth effect, as has been shown. The statistical distribution revealed after removal of the decay trend, discontinuities and distant outliers is consistent with a normal distribution.

In Part 2,¹³ We address the problems in analysis and correlation raised by this work. One key issue raised is what kind of information can be obtained on *component* statistical contributions, and what practical value is afforded by such information.

Acknowledgements

We acknowledge R. J. Garrett and D. C. Creagh for helpful discussions. This work was performed at the Australian National Beamline Facility with support from the Australian Synchrotron Research Program, which is funded by the Commonwealth of Australia under the Major National Research Facilities program.

REFERENCES

1. Rizzuto C. (ed.). *Elettra Highlights (1997)*. Stella Arti Grafiche: Trieste, 1998.
2. Gluskin E, Alp EE, McNulty I, Sturhahn W, Sutter J. *J. Synchrotron. Radiat.* 1999; **6**: 1065.
3. Wark J. *Acta Crystallgr.* 1999; Suppl. K13.04.001.
4. Nikitenko SG, Tolochko BP, Aleshaev AN, Kulipanov GN. *J. Phys. IV* 1997; **7**: 549.
5. Gauthier C, Solé VA, Mishnev I, Signorato R, Goulan J, Moguiline E. *J. Synchrotron. Radiat.* 1999; **6**: 164; Gauthier C, Goulan G, Feite S, Moguiline E, Braicovich L, Brookes NB, Goulan J. *Physica B* 1995; **208**: 232.
6. Pascarelli S, Neisivs T, Panfilis SD, Bonfin M, Pizzini S, Mackay K, David S, Fontaine A, San Migvel A, Itié JP, Gauthier M, Polian J. *J. Synchrotron. Radiat.* 1999; **6**: 146; Pettifer RF, Borowski M, Loeffen PW. *J. Synchrotron. Radiat.* 1999; **6**: 217; Vlaic G, Andreatta D, Cepparo A, Colavita PE, Fonda E, Michalowicz A. *J. Synchrotron. Radiat.* 1999; **6**: 225; Krappe HJ, Rossner H. *J. Synchrotron. Radiat.* 1999; **6**: 302.
7. Chantler CT, Staudenmann J-L. *Rev. Sci. Instrum.* 1995; **66**: 1651.
8. Cookson D. *J. Synchrotron. Radiat.* 1998; **5**: 1375.
9. Chantler CT, Barnea Z, Tran C, Tiller J, Paterson D. *Opt. Quantum Electron.* 1999; **31**: 495.
10. Abramowitz M, Stegun IA (eds). *Handbook of Mathematical Functions*. Dover: New York, 1970; 978–983, Table 26.7.
11. Ito K (ed.). *Encyclopedic Dictionary of Mathematics* (2nd edn). MIT: Cambridge, MA, 1987; 1503–1507, 1816–1819.
12. Chantler CT. *J. Phys. Chem. Ref. Data* 1995; **24**: 71.
13. Chantler CT, Tran CQ, Paterson D, Cookson DJ, Barnea Z. *X-Ray Spectrom.* 2000; **29**: 000.